ISSN 0915-633X

NATIONAL INSTITUTE FOR FUSION SCIENCE

X-Ray Enhancement of SN 1987A Due to Interaction with its Ring-like Nebula

K. Masai and K. Nomoto

(Received – Nov. 4, 1993)

NIFS-265 Dec. 1993

RESEARCH REPORT
NIFS Series

NAGOYA, JAPAN

X-RAY ENHANCEMENT OF SN 1987A DUE TO INTERACTION WITH ITS RING-LIKE NEBULA

Kuniaki Masai

Service d'Astrophysique, CEN Saclay, 91191 Gif-sur-Yvette Cedex, France
and
National Institute for Fusion Science, Nagoya 464-01, Japan

and

Ken'ichi Nomoto

Department of Astronomy, University of Tokyo, Tokyo 113, Japan

Accepted for publication in *Astrophys. J.*

Keywords: shock wave, rarefaction wave, supernova (SN 1987A), radiation mechanism, radiation spectrum

ABSTRACT

The progenitor of the supernova 1987A, Sk-69 202 probably had lost a few $M_\odot$ in its stellar wind in the past evolutionary track from the red supergiant through the blue supergiant. A part of the mass is thought to form the ring-like nebula surrounding SN 1987A by the interaction with the faster wind in the later blue supergiant stage, and the other must be left outside the ring. In 10-20 yr after the explosion, the expanding ejecta will catch up and collide with the ring. Shocks due to the collision will propagate into and heat up the ejecta, the ring, and the matter outside. The shocked matter will be a thermal X-ray source of temperature of several times 10^7 K, and the X-ray luminosity will reach $(0.4\text{-}1)\times10^{37}$ erg s^{-1} for the ring of $0.03\text{-}0.08M_\odot$. The X-ray emission will last for a few decades with luminosity higher than 10^{36} erg s^{-1} depending also on the density outside the ring. We predict the X-ray spectrum as well as the light curve with hydrodynamical calculations taking into account the light travel effect and the opacity of the unshocked ejecta. The epoch of the flare-up depends on the mass inside the ring, and earlier X-ray observations can give a constraint. We give the relations of the mass with the epoch and the pre-flare luminosity in an analytical way based on the self-similar solutions with nonequipartition in the electron and the ion temperatures. Accordingly, the ROSAT observation in 1991 suggests the collision with the ring in 20 yr after the explosion.

Subject headings: nebulae: supernova remnants - shock waves - interstellar: matter - stars: circumstellar shells - stars: individual (SN 1987A) - stars: supernovae

I. INTRODUCTION

The circumstellar structure of SN1987A has been investigated in various wavelengths (see e.g. Chevalier 1992). Within a few days after the explosion, the circumstellar matter became transparent for the emission in radio wavelengths. Infrared and optical observations had suggested an asymmetry in the distribution of the circumstellar matter. Variabilities observed in soft X-rays could also indicate the asymmetry or the clumpy structure. The asymmetry which had been suggested from these observations may be consequent to the less amount of matter in this side on the line of sight to the supernova.

For about 3 years after the explosion, IUE observed emission lines of B-, Be and Li-like ions of carbon and nitrogen. These ions were produced by a UV flash at the moment of the supernova explosion. The UV flux reached its maximum at around 400 days, and indicated the presence of circumstellar matter at 0.5 lt-yr or greater distance from the supernova. Afterward, in visible wavelengths, the Hubble Space Telescope (HST) (Jakobsen et al. 1991) as well as the European Southern Observatory (ESO) (Wampler et al. 1990) gave images of ring-like circumstellar matter. This ring is identical to the matter observed by IUE, since the radius of the ring is coincident with the location of the matter responsible for the UV lines. ESO and HST also reveal that the axis of the ring inclines by about 45° with respect to the line of sight; there is less amount of matter on the line of sight, as suggested by the earlier observations in other wavelengths.

It has been proposed by many authors that the progenitor of SN 1987A had been a red supergiant (RSG) and evolved to be a blue supergiant (BSG) exploding eventually (Saio et al, 1988a,b; Woosley 1988; Weiss 1989; Langer et al. 1989; Tuchman and Wheeler 1991; Yamaoka et al. 1991; Arnett et al. 1989; Hillebrandt and Höflich 1989). The ring structure could be formed by the interaction of the stellar wind of the BSG with the earlier wind of the RSG. The BSG wind with a faster velocity could catch up with the RSG wind matter expanding with a slower velocity. Two shocks arising from the wind-wind collision could propagate from the contact interface into the BSG wind and into the RSG wind remnant, respectively. The shock propagating inward into the BSG wind could cause a turbulent structure behind the shock front. The soft X-rays and their variability observed by Ginga (Inoue et al. 1991) might be related to such matter in clumpy structure (Masai et al. 1988). On the other hand, the shock outward could form a dense shell into the RSG wind matter. The dense shell should be partially photoionized by the UV flash to be bright like a planetary nebula, as taken by HST. It is, however, still open to question how the wind interaction formed the ring-like structure. This may be a question not only to SN 1987A but to ring nebulae observed around AGB stars. Some models have been proposed (Kahn and West 1985; Luo and McCray 1991b; Wang and Mazzali 1992), but further studies are needed (e.g. see Lundqvist 1992; Eriguchi et al. 1992).

If the ejecta envelope is expanding with a velocity of a few times 10^9 cm s^{-1} as suggested by the explosion

models, it will collide with the ring in 10-20 years after the explosion. The shock waves will propagate into and heat up the ring and the ejecta. Thermal X-rays from the shocked matter will rapidly increase and the luminosity will exceed 10^{36} erg s^{-1} (Masai and Nomoto 1991; Luo and McCray 1991a, b; Itoh, Masai and Nomoto 1992; Suzuki, Shigeyama and Nomoto 1993). This enhancement in soft X-rays will last for several decades depending on the mass of the ring and the matter outside, or on the mass loss rate during the RSG stage. X-ray probing of the RSG wind matter will give information on the formation of the ring, the process of the wind-wind interaction, and the chemical composition which may be a clue for understanding the blueward transition of Sk-69 202.

On the basis of the above picture, we predict the epoch and the luminosity of X-ray enhancement due to the interaction with the circumstellar ring and the RSG wind matter, and discuss the dependence of the enhancement on the quantities of the circumstellar matter. The predictions with 2-D hydrodynamics codes have been made available (Luo and McCray 1991b; Suzuki et al. 1993). We employed primarily a 1-D hydrodynamics (HD) code, of which results can be examined by analytical way, and made a ring-geometry correction based on the UV line data observed by IUE to obtain the emergent radiation. Our interest here is focused more on the properties of X-ray emission expected rather than the dynamics. First we describe the model for HD calculations, and give the results in the following sections. In § V we discuss the quantities which are responsible for the X-ray enhancement in an analytical way, and summarize the prediction in the last section.

II. MODEL FOR HYDRODYNAMICAL CALCULATIONS

The density of the ring is estimated by IUE and HST observations to be $\rho_{ring} \approx 3\text{x}10^4$ amu cm^{-3} or (1-4)x10^4 amu cm^{-3} (Jakobsen et al. 1991; Lundqvist and Fransson 1991). Observation with New Technology Telescope (NTT) gives the electron density of the ring to be $7\text{x}10^3$ cm^{-3} (Wampler et al. 1990). These observations give $M_{ring} \approx 0.03$ - 0.08 $M_\odot$ for the mass of the ring. The intensities of UV lines observed by IUE reached their maxima at around 400 days after the explosion. This gives a lower limit of $5\text{x}10^{17}$ cm for the distance from the supernova to the matter emitting UV lines.

At densities of 10^4 amu cm^{-3} the recombination time of photoionized species is about a few years. Therefore, the epoch of the intensity maximum can be predominantly determined by the light travel effect depending on the geometrical structure. If the circumstellar matter were a spherically symmetric shell, the line intensities could increase linearly up to the maximum in proportion to t/t_{max} at time t, as shown in Fig. 1 (a), where $t_{max} \approx 400$ d is the time at

which the intensity reached its maximum. In practice, however, the intensity came up at about 70 days and evolved approximately as

$$I_{obs}(t) \propto \cos^{-1}\left(1 - \frac{c\,t - R_\theta(1-\cos\theta)}{R_\theta \cos\theta}\right), \qquad (1)$$

where $I_{obs}(t)$ is the light curve to be observed at time t after the explosion and $R_\theta \equiv c\ t_{max}/(1+\cos\theta)$ with the inclination angle θ. As compared in Fig. 1, about 45°-inclined ring geometry can account for the UV light curve observed. This result is consistent with a picture taken by HST. Hence, we estimate the distance to the ring matter to be about 6×10^{17} cm taking the light maximum at 400 d and the inclination angle of 45° into account.

The ring is thought to form by the interaction of the wind of a BSG with the wind matter emitted earlier by a RSG. A shock due to the collision of the two winds may propagate and form a dense rim into the RSG wind matter. The dense rim can be photoionized by the UV flash of the supernova to emit UV lines as observed by IUE and look like a ring-like nebula observed by HST. Then there likely exists unshocked RSG wind matter outside the ring. This matter may be extended in proportion to r^{-2} at a distance r from the supernova, if the wind velocity and the mass loss rate does not change so much during the RSG phase and there is no significant disturbance but the wind-wind interaction afterward. If the RSG had lost its mass at a rate 10^{-6} to 10^{-5} $M_\odot$ yr^{-1} in its stellar wind, the mass of a few $M_\odot$ in total could be emitted during the RSG phase and left around the supernova. A part of this mass could be shocked by the wind-wind interaction afterward to be taken into the ring, and other most of the RSG wind matter is to be left outside. For the matter outside the ring, we assume the density as $\rho_{out}(r) \approx 2(r/1\mathrm{pc})^{-2}$ amu cm^{-3} at a distance r ($>R_{ring}$) from the supernova, where R_{ring} is a radius of the ring. Then the total mass lost by the RSG is $\approx 2.7\ M_\odot$ if the wind matter is extended up to being 0.1 amu cm^{-3} in density comparable to the ambient interstellar/cloud medium, or the mass loss rate $\approx 6.3\times10^{-6}\ M_\odot$ if the wind blew with a constant velocity of 10 km s^{-1}.

The BSG wind matter is likely left inside the ring. Before colliding with ring, the expanding ejecta must interact with this matter. The interaction yields thermal X-rays and decelerates the expanding ejecta. The X-ray luminosity observed before the enhancement can give a constraint on the mass or the density of the matter inside the ring. As of 1991, ROSAT observed no X-rays with energy levels higher than 3×10^{34} erg s^{-1} in luminosity (Trümper 1992). This result may impose an upper limit on the matter inside the ring to be $\approx 6\times10^{-2}\ M_\odot$ in mass or ≈ 80 amu

cm^{-3} in density if it is distributed homogeneously within R_{ring}, as discussed in § V.

Based on the above picture of the circumstellar structure, we have investigated the dynamical evolution of SN1987A remnant and the X-ray emission therefrom using a spherically symmetric hydrodynamics - radiation code. For the ejecta we adopt the SN14E1 model proposed by Shigeyama and Nomoto (1990). The total mass of the ejecta is about 14.6 $M_\odot$ and the kinetic energy is 1×10^{51} erg. The chemical composition of the ejecta envelope is as follows: H = 0.566, He = 0.430, C = 2.11×10^{-4}, N = 1.42×10^{-3}, O = 1.14×10^{-3} and $(1/4)Z_\odot$ for the other heavier elements in mass fraction, where $Z_\odot$ represents the value of solar abundance. For the chemical composition of the circumstellar matter, ring and inside/outside the ring, we assume the same composition as the ejecta envelope of the SN14E1 model.

As mentioned above, the radius of the ring is $\approx 6 \times 10^{17}$ cm with inclination angle $\approx 45°$. On account of this geometry, the X-rays emitted from a different part of the ring must travel different distance to reach us, as observed by IUE for UV lines. In order to take this light travel effect into account for the time evolution to be observed, we convolute the temporal data primarily obtained from the 1-D calculation to the kernel derived from the IUE UV-line analysis (Fig. 1). The X-ray flux to be observed at time $t = t_0 + R(t_0)(1-\cos\theta)/c$ is obtained approximately as

$$F(t) = F\left(t_0 + \frac{R(t_0)}{c}(1 - \cos\theta)\right) = \frac{\displaystyle\int_{t_0 - \frac{2R(t_0)}{c}\cos\theta}^{t_0} F_0(t') \cos^{-1}\left(1 - c\,\frac{t_0 - t'}{R(t_0)\cos\theta}\right) dt'}{\displaystyle\int_{t_0 - \frac{2R(t_0)}{c}\cos\theta}^{t_0} \cos^{-1}\left(1 - c\,\frac{t_0 - t'}{R(t_0)\cos\theta}\right) dt'}, \qquad (2)$$

where t_0 is the time on the 1-D calculation and F_0 is the flux at that moment. The convolution by eq. (2) with a kernel as drawn in Fig. 1 (b) - (e) works as if the radiation sources, which are distributed like a shell in the framework of spherically symmetric calculation, get together uniformly along its equator with the inclination angle θ. The delay between t and t_0 expressed in the left-hand side of eq. (2) reflects the inclination; in the case of $\theta \approx 45°$, the flux comes up at ≈ 70 d after the explosion ($t = 0$), as shown in Fig. 1 (d) and also suggested from IUE UV-lines.

X-rays from the far side are absorbed by the intervening unshocked ejecta. With multiplying an effective solid angle $\omega(r,E)$, this process is taken into account for the emergent flux $F_0(E,t_0)$ in the interval of photon energy dE as

$$F_0(E,t_0) = \int_{r_{in}}^{r_{out}} f_0(r,E,t_0)\ \omega(r,E)\ r^2\,dr\ , \qquad (3)$$

where $f_0(r,E,t_0)$ is the flux from a zone specified by radius r, and r_{in} and r_{out} are the innermost radius of the reverse-shocked ejecta and the outermost radius of the forward-shocked ambient matter, respectively. $\omega(r,E)$ is given by

$$\omega(r,E) = 2\pi\left[1+\sqrt{1-(r_{in}/r)^2}+\frac{1}{r^2}\int_0^{r_{in}}\exp\left(-\frac{2}{x}\int_x^{r_{in}}\sigma(r,E)\frac{n(r)\,r\,dr}{\sqrt{(r/x)^2-1}}\right)\frac{x\,dx}{\sqrt{1-(x/r)^2}}\right], \qquad (4)$$

where $n(r)$ is the density and $\sigma(r,E)$ is the absorption cross section depending on the elemental abundance at a radius r of the ejecta. Absorption by the circumstellar matter is negligible. As to the interstellar matter, absorption by the equivalent hydrogen column is taken into account separately, as mentioned in the next section.

One may notice that neither the convolution kernel in eq. (2) nor the effective solid angle given by eq. (4) includes the correction in the radiation intensity for the solid angle Ω_{ring} covered with the ring. If the density is given for the matter with which the ejecta interacts, such a correction as multiplying $\Omega_{ring}/4\pi$ would be consistent with the mass responsible for the interaction and the resultant emission. In our calculation, however, the mass is defined as an explicit parameter for the circumstellar matter except for the RSG wind outside the ring. Therefore, the intensity is integrated over the whole mass being able to be responsible for. Actually, when the mass is given, the free-free luminosities obtained from our spherically symmetric HD are consistent with those obtained by Suzuki et al. (1993) from 2-D HD modeling, which provides a more realistic geometry of the ring.

We carried out the HD calculations for the cases: (M_{in}, M_{ring}, ρ_{ring}) = (4, 8, 3), (4, 3, 3), (4, 3, 2), (4, 3, 0.7), (8, 3, 0.7) and (2, 3, 0.7) in units of 10^{-3} $M_\odot$, 10^{-2} $M_\odot$ and 10^4 amu cm^{-3}, respectively, where M_{in} is the mass of the BSG wind matter inside the ring. In all cases $\rho_{out} \approx 2(r/1\mathrm{pc})^{-2}$ amu cm^{-3} at $r > R_{ring}$ is assumed for the matter outside the ring. Since the thickness of the ring is not given explicitly, larger ρ_{ring} means the thinner ring for

the same M_{ring}. In the following sections, we describe the interaction and the emission calculated for the case M_{in} = 4×10^{-3} $M_\odot$, $M_{ring} = 3\times10^{-2}$ $M_\odot$ and $\rho_{ring} = 0.7\times10^{4}$ amu cm^{-3}, referring as well to the results of other cases.

III. TIME EVOLUTION OF INTERACTION

The dynamical evolution is shown in Fig. 2 (a), where the radii to bound the ejecta, matter inside the ring (BSG wind matter), the ring and the matter outside (RSG wind matter) are drawn together with r_{in} and r_{out} as functions of time. The supernova ejecta expand compressing the BSG wind matter bounded by the ring. The blast shock from the supernova ejecta hits the ring at around 12 yr and compresses the ring as well. Since the ring is so thin, as $\approx 10^{15}$ cm in the spherically symmetric HD here, the shock soon breaks out of the ring forward into the RSG wind matter of lower density. The resultant rarefaction wave propagates backward into and cools adiabatically the ring; it should be noticed that such rarefaction is important in the interaction with a dense clump in the free expansion phase, and works on cooling much more rapidly than radiation (e.g. Masai et al. 1988). The reverse shock propagating inward is reflected by the ejecta, and propagates outward again into and reheats the ring. These processes are repeated many times decreasing the practical amplitude with expanding the ring. The reverse shock heats up also the ejecta envelope. At about 15 yr the reverse shock propagates further into and heats the ejecta. This enhances the fluorescence Kα-lines of iron and hard X-rays, as seen in the spectrum at 17 yr of Fig. 5 (b).

Fig. 2 (b) shows the thermal energy contained in the ejecta, the matter inside the ring, the ring and the matter outside, respectively. One can see the above processes in the time evolution of the thermal energy. To see the influence of the dynamics shown in Fig. 2 on the radiation shown in Figs. 3 - 5, one must recall the delay due to the light travel effect discussed in § II. It should be also noted that the thermal energy contained in each matter is not linearly reflected by the radiation therefrom. Though the thermal energy of the ring is much smaller than that of the other circumstellar matter, the thermal emission from the ring is larger because of its much higher density. In cooperation with a magnetic field thermal energy can be responsible for acceleration of charged particles to result in emission of high energy γ-rays.

Shown in Fig. 3 (a) is the time evolution of the *apparent* luminosity in the range from 0.2 to 20 keV, where *apparent* means that the light travel effect and the intrinsic absorption by the unshocked ejecta are taken into account, as described in § II. The X-ray enhancement due to interaction with the ring and the matter outside will last for several decades with the luminosity higher than 10^{36} erg s^{-1}. The epoch of the enhancement depends not only on the location of the ring but also the amount of the matter inside, as mentioned in § I. The mass inside the ring is also responsible

for the X-ray luminosity before the enhancement, which can give information for the epoch of the enhancement following. In this sense, it is of practical interest how the earlier light curve depends on the mass inside the ring. For illustrative purpose, the early light curves are shown in Fig. 3 (b) for the three cases, M_{in} = 8×10^{-3} $M_\odot$, 2×10^{-3} $M_\odot$ and 4×10^{-3} $M_\odot$. The processes taken into account and the parameters but M_{in} are the same in all three cases. The dependence of M_{in} on the epoch of the flare and the pre-flare luminosity is discussed further in § V.

The X-ray flux expected at the earth is shown in Fig. 4, where the distance of 52 kpc to the supernova and the interstellar absorption equivalent to hydrogen column density of 2×10^{21} N_H cm^{-2} with solar abundances are assumed in addition to absorption by the unshocked ejecta. The two energy bands, 0.2-2 keV and 2-20 keV, are chosen to demonstrate a contrast in their time evolutions. The 0.2-2 keV flux rapidly rises to reach its maximum in several years, while the 2-20 keV flux increases gradually. As shown later, this contrast may come from a difference in emission processes contributing to the two energy bands; below 2 keV, the line emission due to L-shell excitation is dominant whereas the free-free continuum dominates above 2 keV. In Fig. 4, also the light curve obtained straightforwardly from the spherically symmetric calculation is also shown to demonstrate the light travel effect. The spikes in the beginning are due to the reflections of the shock wave between the two contact interfaces of the ring, as described above. One can see that the convolution process with the light travel effect lets the spikes diffuse and the epoch of the enhancement delay by about a year.

IV. PROPERTIES OF THERMAL X-RAYS

We calculate the X-ray spectrum from the shocked matter taking into account nonequilibrium ionization as well as nonequipartition in thermal energy of protons and electrons. Free-free, free-bound up to n = 3 levels of H-, He- and Li-like ions, two photon decay from n = 2 metastable levels of H- and He-like ions, and line transitions are considered for the 15 elements, H, He, C, N, O, Ne, Na, Mg, Al, Si, S, Ar, Ca, Fe and Ni with their elemental abundances described in § II. Fluorescence following innershell ionization, cascade following radiative recombination and innershell excitation as well as excitation from ground states and dielectronic recombination satellites are taken into account for line transitions in nonequilibrium ionization. Collisional innershell ionization - fluorescence and recombination - cascade play important roles in line emission in compression waves and rarefaction waves, respectively (Masai 1993), as demonstrated for the shock wave breaking out of the dense circumstellar matter (Itoh and Masai 1989). This is the case also for the interaction of SN 1987A with the ring, as the dynamics is described in § III.

The contribution of each emission process above can be seen in Fig. 5 (a), which shows the X-ray spectrum at about 22 yr after the explosion. Here the total emission and the line emission are convoluted to a Gaussian kernel with FWHM = 0.18E at a photon energy E keV. The distance 52 kpc to the supernova with interstellar absorption of $2x10^{21}$ N_H cm^{-2} is taken into account as well. The X-ray emission in the 0.2-2 keV range is dominated by the prominent lines due to K-shell transitions of C, N and O and L-shell transitions of heavier elements. With the energy resolution taken here, these lines are not resolved but are blended to an enhancement with a peak around 0.5-0.8 keV. K-shell transitions of Si, S, Ar, Ca, Fe and Ni can be distinguished from each other. But, the line of each element is also blended with many transitions unresolved.

Fig. 5 (b) shows the snap shots of the spectra in course of the interaction. Also the time evolution of iron Kα-line blend (n = 1-2 transitions including their satellites of various ionic states) is shown with its equivalent width and mean energy weighted with each line emissivity. In the calculation here, the Doppler shift due to expansion is not taken into account. It takes $\approx 3(\rho/10^4$ amu $cm^{-3})^{-1}$ yr for the shocked matter to reach an ionization equilibrium (Masai 1993). Nonequilibrium ionization affects the spectra at energies substantially below 2 keV, where the line emission dominates. At energies above 2 keV, free-free emission dominates the whole spectrum. Since the free-free emission is dominated by abundant species of low ionization potentials such as H and He, the emissivity is almost free from nonequilibrium ionization and follows immediately the increase in the electron temperature. During the X-ray enhancement, an average temperature weighted by the free-free volume emissivity is in a range of a few 10^7 K, though the free-free spectrum can not be reproduced by the single temperature. K-lines of elements such as Si, S, Ar, Ca, Fe and Ni are subject to nonequilibrium. One can notice that L-shell and K-shell lines of iron coexist in a spectrum. In the 17-yr spectrum where the L-line is enhanced, the K-line also is enhanced at an energy lower than the later ones; the K-line emission is characterized by innershell processes.

In the rising phase of the X-ray luminosity through about 14 yr, K-lines of carbon and oxygen still dominate the emission below 1 keV. Afterward metal L-lines, e.g. Ne-like iron Fe XVII 2p (^{1}S) - 3d (^{1}D) and its satellites, take the place to enhance the emission at around 0.8 keV. Most of these X-rays below 1 keV comes from the blast-shocked circumstellar matter. The X-rays above 2 keV rise behind those below 0.2 keV and the higher energy spectrum due to free-free emission reaches its maximum hardness at around 20 yr. A few years later, the mean energy of the iron Kα-line reaches its maximum because of nonequilibrium ionization as mentioned above. Through about 18 yr, the line emission is dominated by innershell excitation/ionization of ions keeping L-shell electrons. This results in the mean line energy to be lower than 6.63 keV of the He-like forbidden line (1s (^{1}S) - 2s (^{3}S)), which is produced by excitation from the ground state of He-like as well as fluorescence following innershell ionization of Li-like ions. The equivalent width reaches its maximum to be about 240 eV at around 22 yr.

When a supernova explodes into a medium where the density is uniform or monotonically distributed, in the early phase up to the dynamical time scale, the X-ray emission from the supernova remnant is dominated more by that from the reverse-shocked ejecta envelope than the shocked ambient matter. Here the dynamical time scale may be defined by the time at which the mass of the swept-up ambient matter becomes comparable to the initial ejecta mass, or by the time at which the reverse shock propagating into the ejecta reaches its core. The above case may be attained for the early X-ray emission from SN 1993J, if the progenitor is surrounded by its past stellar wind as expressed simply by $\rho \propto r^{-2}$. In the interaction of SN 1987A with the circumstellar matter including the ring, however, this is not the case but the X-ray emission from the shocked circumstellar matter can be comparable to or exceed that from the shocked ejecta envelope, though SN 1987A is too young for the reverse shock to propagate into the ejecta core.

V. DISCUSSION

The epoch and the characteristics of the X-ray enhancement depend on the quantities of the circumstellar matter, such as M_{in}, M_{ring} ρ_{ring}, ρ_{out} and so on, and the ejecta model. The X-ray luminosity at the flare-up depends substantially on the mass of the ring, and can be approximately estimated as $L_X \approx 3\times10^{38}\ (M_{ring}/M\odot\ )^{6/5}$ for $\rho_{ring} \approx 10^4$ amu cm^{-3}. Suzuki et al. (1993) give an empirical scaling for the maximum luminosity based on 2-D HD, as $L_{max} \approx 4.2\times10^{38}\ (M_{ring}/M\odot\ )^{1.34}\ (\rho_{ring}/10^4$ amu cm$^{-3})^{0.53}$. In the former, line, free-bound and 2γ-decay emission as well as free-free emission, and absorption by unshocked ejecta are taken into account, while in the latter only free-free emission is taken into account without absorption. In both cases the SN14E1 model is applied for the ejecta. Within the estimates of $M_{ring} \approx 0.03$ - 0.08 M$\odot$ so far, the both estimations of the luminosity fall in the same range of (0.4-1.4)x10^{37} erg s^{-1} for $\rho_{ring} \approx 10^4$ amu cm^{-3}.

Compared to the quantities of the ring, which are deduced from observations, the quantities of the matter inside are quite uncertain. We here discuss the interaction of the ejecta with the matter inside to get the M_{in} dependence of the epoch of the X-ray enhancement and the pre-flare luminosity, which will be useful to forecast the enhancement following. For the interaction concerned, only the envelope of the ejecta can be responsible, and its steepness affects the quantities in the reverse shock and the blast shock. With the density distribution $\rho_{ej} = t^{-3}(r/tU_c)^{-n}$ for the ejecta envelope ($n > 5$), self-similar solutions are found by Chevalier (1982) for the two shocks. The interaction with the matter inside the ring decelerates the ejecta expanding. The time when the blast shock reaches to

strike the ring is given by the self-similar solution depending on the ejecta model as well as M_{in} (Chevalier and Liang 1989; Luo & McCray 1991b). With the density being constant at $r < R_{ring}$, the epoch of the collision is estimated as,

$$t_{ring} \approx 14 \left(\frac{M_{in}}{10^{-2}M_\odot}\right)^{1/6} \left(\frac{U_c}{3.4\text{x}10^9}\right)^{-3/2} \left(\frac{R_{ring}}{6\text{x}10^{17}\text{cm}}\right) \text{ yr} , \qquad (5)$$

hereafter $n = 9$ is assumed; the envelope of SN14E1 gives $n \approx 8.6$. The X-ray flare-up will delay from t_{ring} given by eq. (5) by about a year due to the light travel effect discussed in § II.

If there exists no collective mode excited through the magnetic field, the ions are heated within the shock and their energies are transferred to electrons through Coulomb collisions in the post-shock region. Taking this process into account, Masai (1993) derives the electron temperatures and the free-free luminosities for the blast and the reverse shocks based on the self-similar analysis. The results give the electron temperatures, as

$$T_{eb} \approx 4.4\text{x}10^7 \left(\frac{M_{in}}{10^{-2}M_\odot}\right)^{14/45} \left(\frac{U_c}{3.4\text{x}10^9}\right)^{4/5} \left(\frac{R_{ring}}{6\text{x}10^{17}\text{cm}}\right)^{-14/15} \left(\frac{t}{10\text{yr}}\right)^{2/15} \text{K} , \qquad (6)$$

for the blast shock and $T_{er} \approx 0.83\ T_{eb}$ for the reverse shock. Here the mass density inside the ring $\approx 1.8 m_H n_H$, the electron number density $\approx 1.4 n_H$ and the mean molecular weight ≈ 0.68 according to the elemental abundance described in § II, where m_H and n_H are the mass and the number density, respectively, of hydrogen. The free-free luminosity both from the blast and the reverse shocks is obtained, as

$$L^{FF} \approx 1.6\text{x}10^{34} \left(\frac{M_{in}}{10^{-2}M_\odot}\right)^{82/45} \left(\frac{U_c}{3.4\text{x}10^9}\right)^{17/5} \left(\frac{R_{ring}}{6\text{x}10^{17}\text{cm}}\right)^{-82/15} \left(\frac{t}{10\text{yr}}\right)^{31/15} \text{erg s}^{-1} . \qquad (7)$$

A correction factor to eq. (7) for the X-ray photons in the 0.2-20 keV range is around 0.9 at $T_e \approx$ a few 10^7 K. The line emission is subject to nonequilibrium ionization because t_{ring} is still smaller than the ionization time scale (Masai 1993). If equilibria were attained, taking into account the elemental abundances described in § II, we would have the line luminosity at t_{ring}, as

$$L_X^L \approx 6\text{x}10^{32}\left(\frac{M_{in}}{10^{-2}M_\odot}\right)^{5/3}\left(\frac{U_c}{3.4\text{x}10^9}\right)^{-3/5}\left(\frac{R_{rng}}{6\text{x}10^{17}\text{cm}}\right)^{-11/5} \text{ erg s}^{-1} ,$$

in the 0.2-20 keV range. The line luminosity may be larger in nonequilibria by a factor, which decreases with increasing M_{in}. At $t < t_{ring}$ the line luminosity does not likely exceed this value, since the line luminosity in equilibria varies $\propto t^{28/15}$ although the emissivity is enhanced with ionizing.

The above analysis is valid after the maximum light through $t < t_{ring}$. The values obtained for $M_{in} \approx 4\text{x}10^{-3}$ M $\odot$ and the dependence are fairly in good agreement with the HD calculation. In 1991 ROSAT obtained the upper limit $\approx 3\text{x}10^{34}$ erg s^{-1} on the luminosity (Trümper 1992). Eq. (6) gives the electron temperatures of a few 10^7 K for the blast and the reverse shocks at $t \approx 4$ yr. Then, with a correction factor ≈ 0.5 to eq. (7) for the observation energy band of ROSAT (0.1-2.4 keV), we have an upper limit $M_{in} < 6\text{x}10^{-2}$ M$\odot$ for the mass inside the ring. The ROSAT observation gives a constraint also on the epoch of the X-ray enhancement. Using eq. (5), we have a limit $t_{rng} < 19$ yr, i.e., the X-ray flare-up will be observed in about 20 yr after the explosion. In addition, if the density inside the ring is likely higher than 1 amu cm^{-3}, the epoch is probably in a range from 10 to 20 yr.

VI. SUMMARY AND REMARKS

The expanding ejecta of SN 1987A will collide with the ring in 10-20 yr after the explosion depending on the mass inside. The resultant shocks will propagate into and heat up the ejecta envelope and the ring to cause a soft X-ray enhancement. An associated rarefaction wave will cool the shocked ring adiabatically and the reflected shock wave reheat it. This repeated processes may be observed as a fluctuation of the X-ray intensity in the early light curve. The X-ray luminosity will reach (0.4-1)x10^{37} erg s^{-1} for the ring of 0.03-0.08 M$\odot$. The enhancement initiated by the collision with the ring will last for a few decades with luminosity higher than 10^{36} erg s^{-1} depending also on the thickness of the ring and the distribution of the matter outside.

The thermal emission can be expected also in other wavelengths, ultraviolet, optical, infrared and radio (Luo & McCray 1991a, b). There may also be radio and high energy γ-rays due to non thermal particles associated with shocks. The propagating shock wave will be a probe to diagnose the circumstellar structure, the BSG wind, the ring

and the RSG wind, with expanding the ejecta. The observations will give some clue for understanding the wind-wind interaction and the ring formation. The earlier observations can give a constraint on the mass of the BSG wind matter inside the ring as well as to forecast the flare-up. Continual observations are desired to improve the upper limits on M_{in} and t_{ring}, as discussed in the last section.

Apart from the uncertainty in the quantities of the circumstellar matter, the following questions still remain to be discussed.

(i) Suzuki et al. (1993) based on 2-D HD show a much slower increase in the 0.2-2 keV luminosity in the collision with the ring than with the spherical shell. Our calculation is based on spherically symmetric HD although the geometrical effect of the ring on the emergent radiation is taken into account in the post process. On the other hand, the former ignores the line emission which should rise in the first mainly below 2 keV, as seen in Fig. 5 (b). In the 2-20 keV flux predominantly due to free-free emission, our calculation also gives as slow an increase as Suzuki et al., which shows no appreciable difference between the ring and the shell. However, Luo & McCray (1991b) based on 2-D HD shows a faster increase in X-rays < 3.5 keV than in > 3.5 keV, but slower than their previous 1-D HD (Luo & McCray 1991a). From these comparisons, we cannot exclude the possibility that the X-ray luminosity may increase more slowly than predicted in the present work, in relation also with the following question.

(ii) As discussed in § II, we calculate the radiation for the responsible mass to be consistent with the realistic structure. In the argument in § V we choose not density but M_{in} as a parameter for the matter inside the ring. If the realistic structure is far from the spherically symmetric configuration, M_{in} does not represent all the mass in a sphere of radius R_{ring} but should be read as an amount which is practically responsible for the interaction and the resultant radiation; the matter within Ω_{ring} likely gives a larger contribution than the matter far outside. In the case of the ring, the mass and the density given must be linked with a geometrical parameter of thickness. The radial thickness of the ring $\propto \Omega_{ring}^{-1} (M_{ring}/\rho_{ring})$ would be smaller in the spherically symmetric HD than the realistic geometry. This is the most serious issue in the spherically symmetric HD and may be influential on the light curve, though the integrated radiation is not altered but determined predominantly by M_{ring}.

(iii) The density outside the ring can influence the long-term light curve. In the calculation here, we assume the RSG wind matter being adjacent to the ring outside. However, outer loops of the circumstellar matter are found to have much greater dimensions than the ring, and are likely related to the inner boundary of the RSG wind matter. The presence of another medium between the ring and the loops may alter the light curve predicted, yet the luminosity at the flare-up is little influenced.

(iv) We treat all the matter being in the gas phase. Observations suggest the dust formation in the ejecta, and also a part of the matter of the RSG wind is likely in a form of dust. If it is the case, nonequilibrium ionization is

more enhanced (Itoh 1988), and thus the resultant X-ray emission could be affected at the initial phase of the interaction. Itoh et al. (1992) take into account the processes in the gas-dust mixture and predict the enhancement in infrared wavelengths as well as X-rays.

The authors would like to thank H. Itoh and R. McCray for their invaluable comments. K. M. is grateful to C. Cezarsky, M. Arnaud and their colleagues for their hospitality at Service d'Astrophysique, CEN Saclay, and also to S. Hayakawa for his encouragement for astrophysics.

References

Arnett W.D., Bahcall J.N., Kirshner R.P., and Woosley S.E., 1989, AR A&A 27, 629.

Chevalier R.A., 1982, Ap. J. 259, 302.

Chevalier R.A., and Liang E.P., 1989, Ap. J. 344, 332.

Chevalier R.A., 1992, Nature 355, 691.

Eriguchi Y., Yamaoka H., Nomoto K., and Hashimoto M., 1992, Ap. J. 392, 243.

Hillebrandt W., and Höflich P., 1989, Rep. Prog. Phys. 52, 1421.

Inoue H., Hayashida K., Itoh M., et al., 1991, PASJ 43, 213.

Itoh H., and Masai K., 1989, MNRAS 236, 885.

Itoh H., 1988, PASJ 40, 263.

Itoh H., Masai K., and Nomoto K., 1992, *Frontiers of X-Ray Astronomy* (eds. Tanaka Y., Koyama K.), Universal Acad. Press, Tokyo, p. 383.

Jakobsen P., Albrecht R., Barbieri C., et al., 1991, Ap. J. 369, L63.

Kahn F.D., and West K.A., 1985, MNRAS 212, 837.

Langer N., El Eid M.F., and Baraffe I., 1989, A&A 224, L17.

Luo D., and McCray R., 1991a, Ap. J. 372, 194.

Luo D., and McCray R., 1991b, Ap. J. 379, 659.

Lundqvist P., 1992, PASP, 104, 787.

Lundqvist P., and Fransson C., 1991, Ap. J. 380, 575.

Masai K., Hayakawa S., Inoue H., Itoh H., and Nomoto K., 1988, Nature 335, 804.

Masai K., and Nomoto K., 1991, *Supernovae* (ed. Woosley S.E.), Springer, Berlin, p. 153.

Masai K., 1993, submitted to Ap. J.

Saio H., Kato M., Nomoto K., 1988a, Ap. J. 331, 388.

Saio H., Nomoto K., Kato M., 1988b, Nature 334, 508.

Shigeyama T., and Nomoto K., 1990, Ap. J. 360, 242.

Suzuki T., Shigeyama T., and Nomoto K., 1993, A&A 275, 883.

Tuchman Y., and Wheeler J.C., 1991, *Supernovae* (ed. Woosley S.E.), Springer, Berlin, p. 159.

Trümper J., 1992, *Frontiers of X-Ray Astronomy* (eds. Tanaka Y., Koyama K.), Universal Acad. Press, Tokyo, p. 185.

Wang L., and Mazzali P.A., 1992, Nature 355, 58.

Weiss A., 1989, Ap. J. 339, 365.

Woosley S.E., 1988, Ap. J. 330, 218.

Yamaoka H., Saio H., Nomoto K., Kato M., 1991, IAU Symp. 143 *Wolf-Rayet Stars and Interrelations with Other Massive Stars in Galaxies* (eds. Van der Hucht K., Hidayat B.), Kluwer, Dordrecht, p. 571.

Figure Captions

Fig. 1 Time evolution of the radiation flux expected with the light travel effect from the matter distributed as (a) spherically symmetric shell, (b) edge-on ring (0°-inclination), (c) 30°-inclined ring, (d) 45°-inclined ring and (e) 60°-inclined ring with respect to the line of sight. The flux is assumed to be its maximum at 400 d in every case.

Fig. 2 Hydrodynamical evolution of the interaction between the ejecta and the circumstellar matter: (a) time variation of the radius of each contact interface of the ejecta, the matter inside the ring (BSG-W), the ring and the matter outside (RSG-W), and (b) time evolution of the thermal energy contained in each matter.

Fig. 3 Time evolution of 0.2-20 keV luminosity: (a) long-term variation in case of $4\times10^{-3}M_{\odot}$ and (b) flare-up phase expanded in cases of $2\times10^{-3}M_{\odot}$, $4\times10^{-3}M_{\odot}$ and $8\times10^{-3}M_{\odot}$ for the mass inside the ring. Light travel effect is taken into account by convoluting the temporal emissivity to the curve of Fig. 1(d). Also is taken into account the absorption of the X-rays from the other side through the unshocked ejecta.

Fig. 4 X-ray flux in 0.2-2 keV and 2-20 keV at a distance of 52 kpc from the supernova. Interstellar absorption equivalent to 2×10^{21} N_H cm^{-2} with solar abundances is taken into account. The solid lines and the broken lines represent the cases with and without the light travel effect, respectively.

Fig. 5 X-ray spectra at a distance of 52 kpc with interstellar absorption of 2×10^{21} N_H cm^{-2}: (a) contribution of each emission process at ≈ 22 yr after the explosion, and (b) time evolutions of the whole spectrum and the iron Kα-line. The spectra except for the contributions of the continua are convoluted to a Gaussian kernel with FWHM=0.18E (keV).

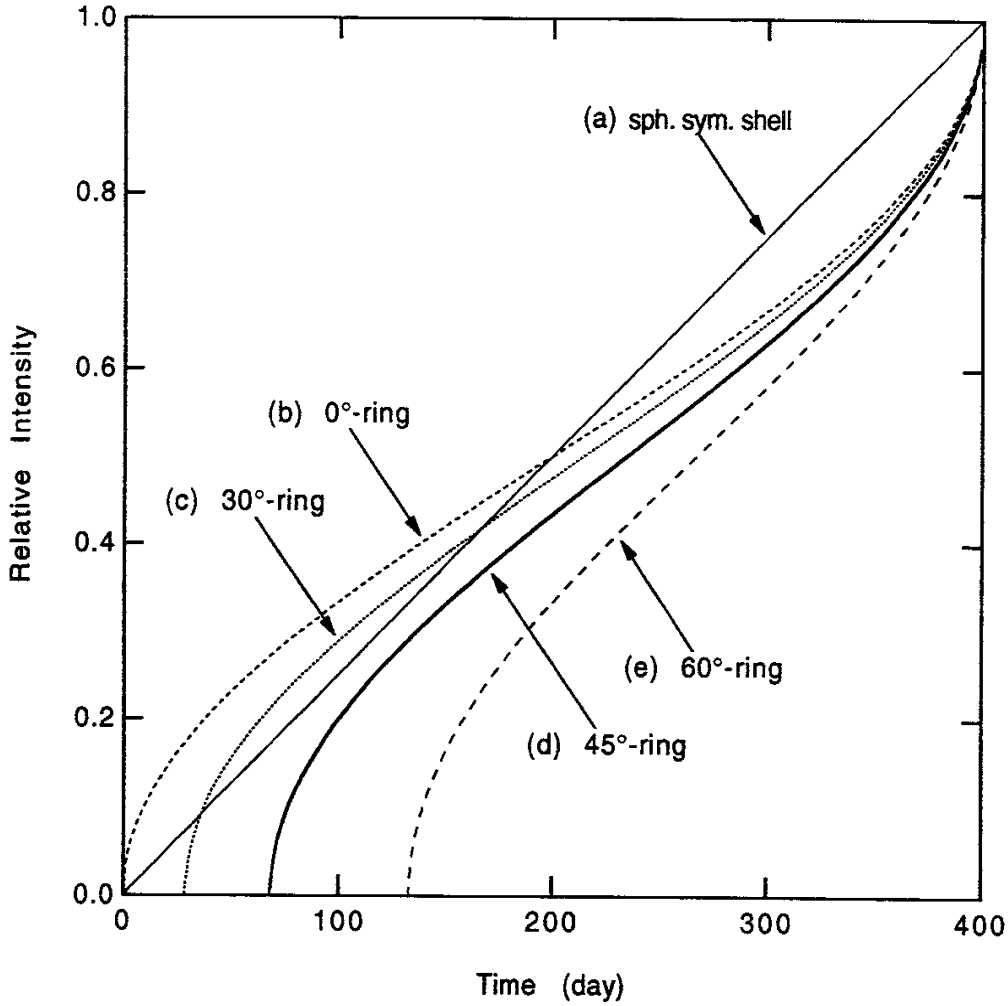
1.0
0.8
0.6
0.4
0.2
0.0
Relative Intensity
0
100
200
300
400
Time (day)
(a) sph. sym. shell
(b) 0°-ring
(c) 30°-ring
(d) 45°-ring
(e) 60°-ring

Fig. 1

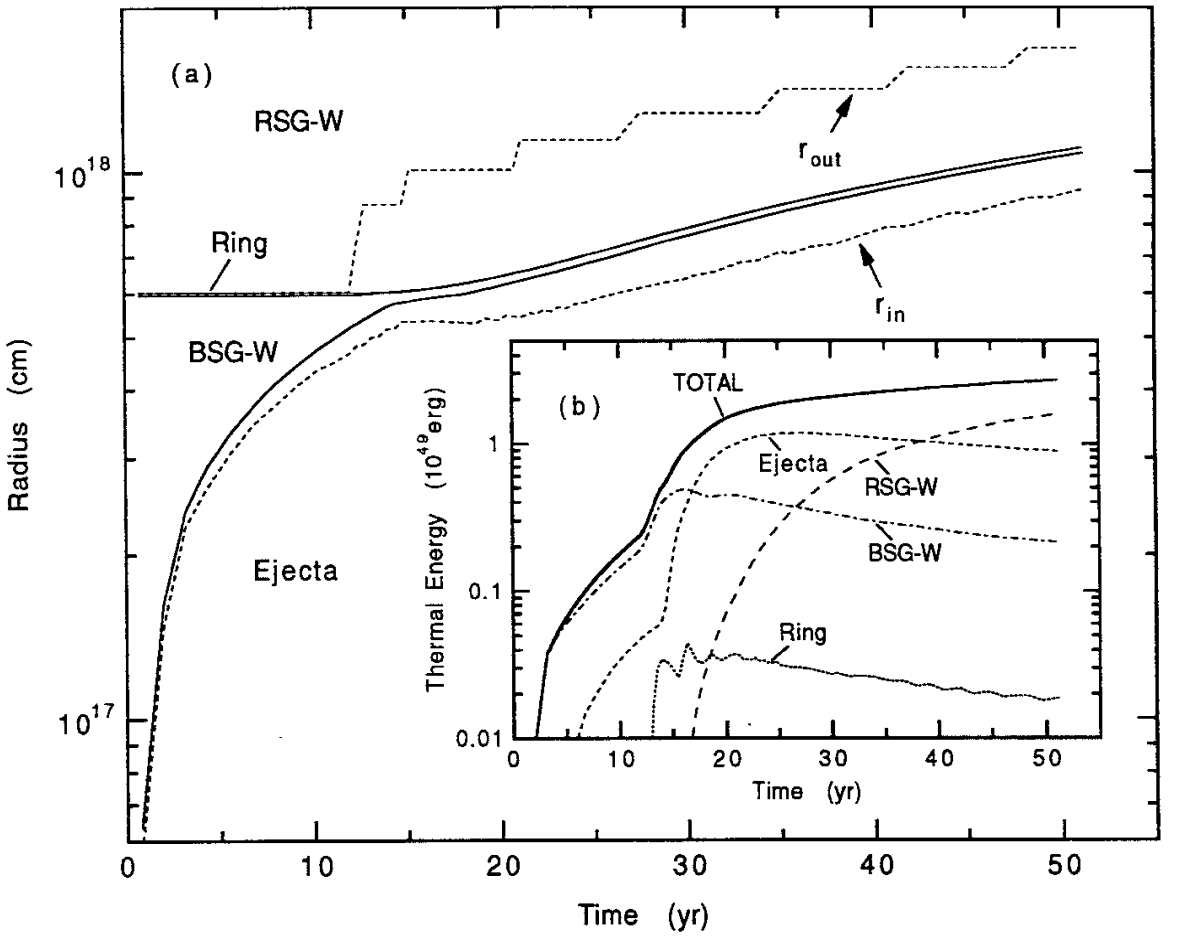
(a)
RSG-W
Ring
BSG-W
Ejecta
r_{out}
r_{in}
10^{18}
10^{17}
Radius (cm)
0
10
20
30
40
50
Time (yr)
(b)
TOTAL
Ejecta
RSG-W
BSG-W
Ring
Thermal Energy (10^{49}erg)
1
0.1
0.01
0
10
20
30
40
50
Time (yr)

Fig. 2

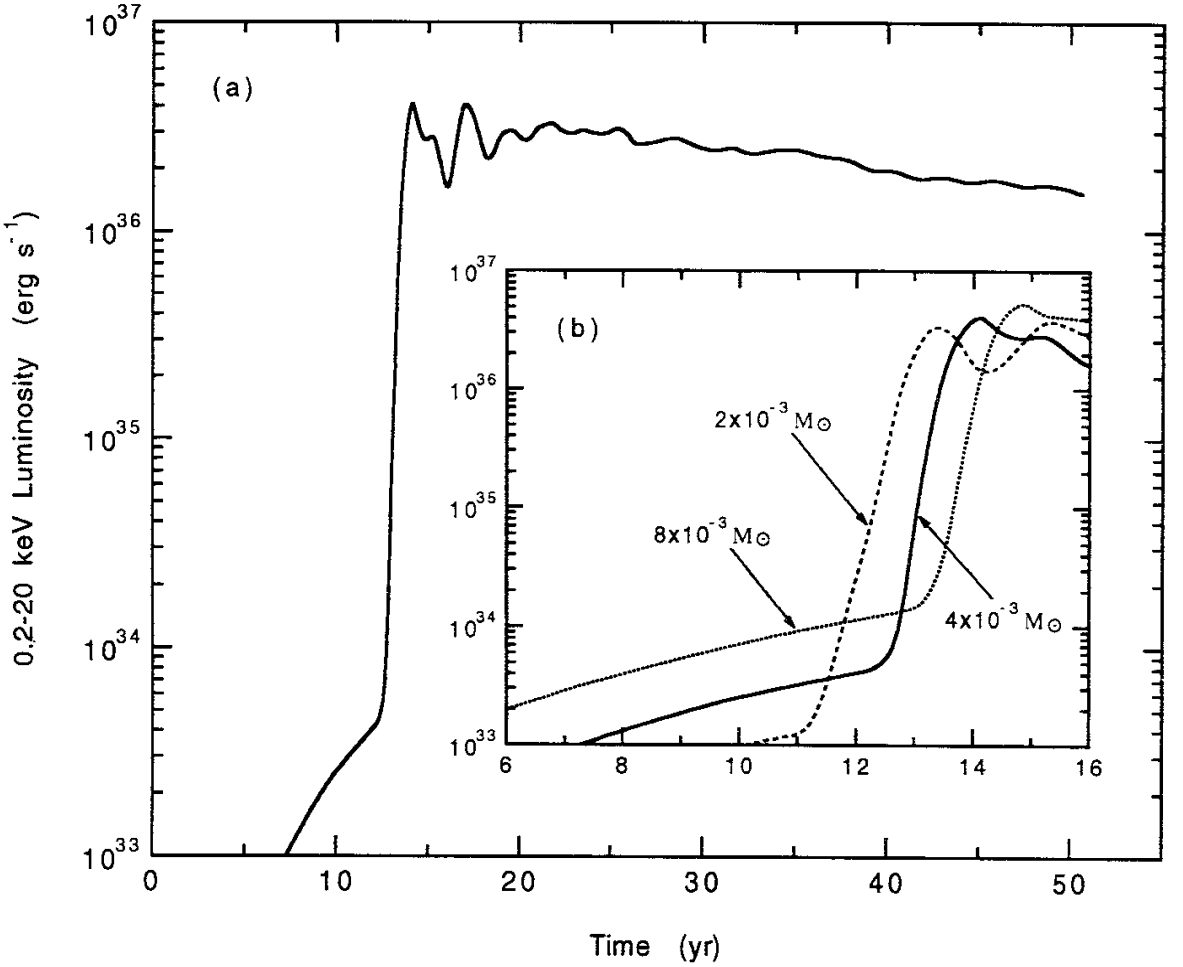
(a)
(b)
0.2-20 keV Luminosity (erg s^{-1})
Time (yr)
10^{37}
10^{36}
10^{35}
10^{34}
10^{33}
0
10
20
30
40
50
6
8
10
12
14
16
2x10^{-3} M$\odot$
8x10^{-3} M$\odot$
4x10^{-3} M$\odot$

Fig. 3

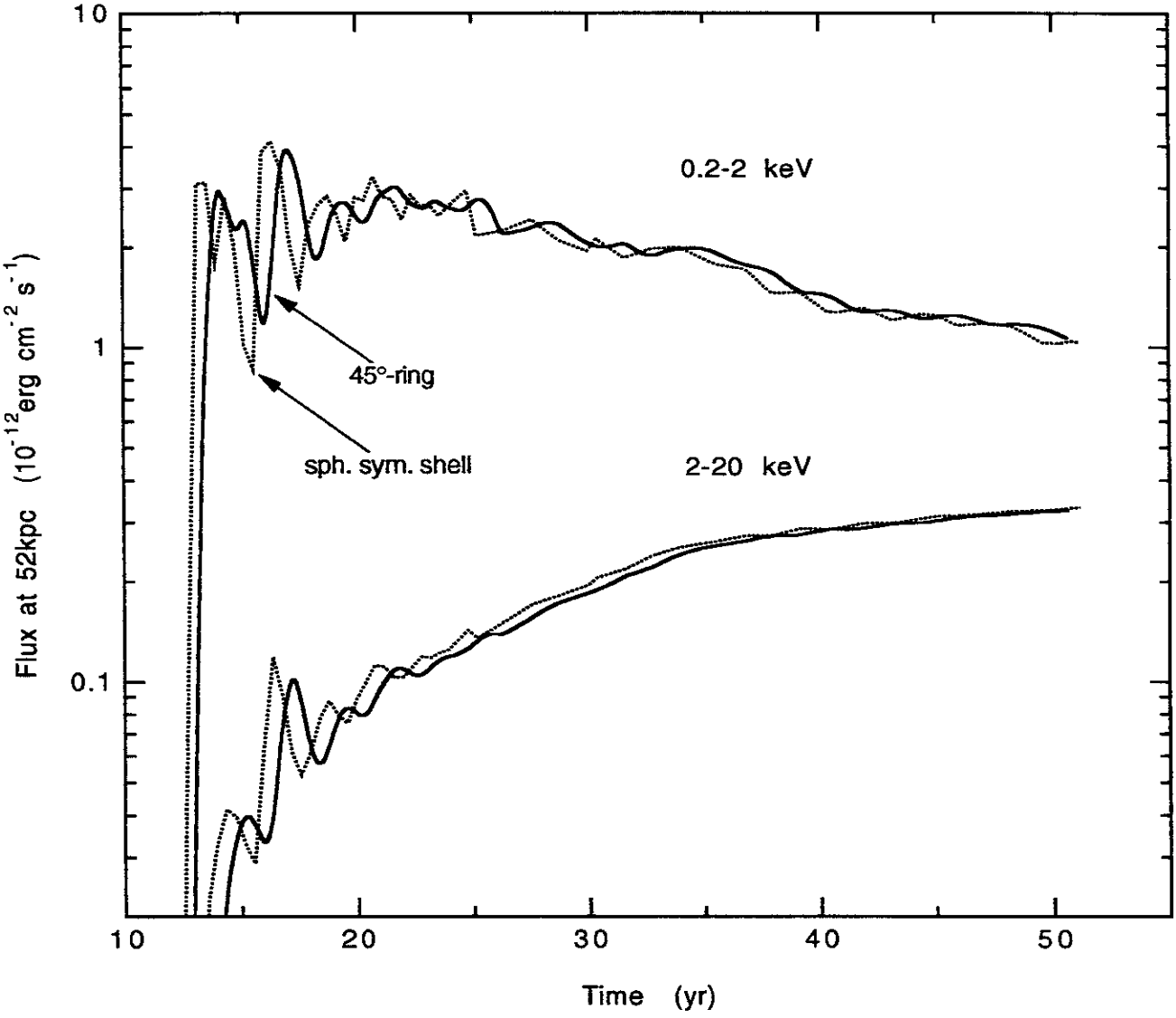
10
1
0.1
10
20
30
40
50
Time (yr)
Flux at 52kpc (10^-12 erg cm^-2 s^-1)
0.2-2 keV
2-20 keV
45°-ring
sph. sym. shell

Fig. 4

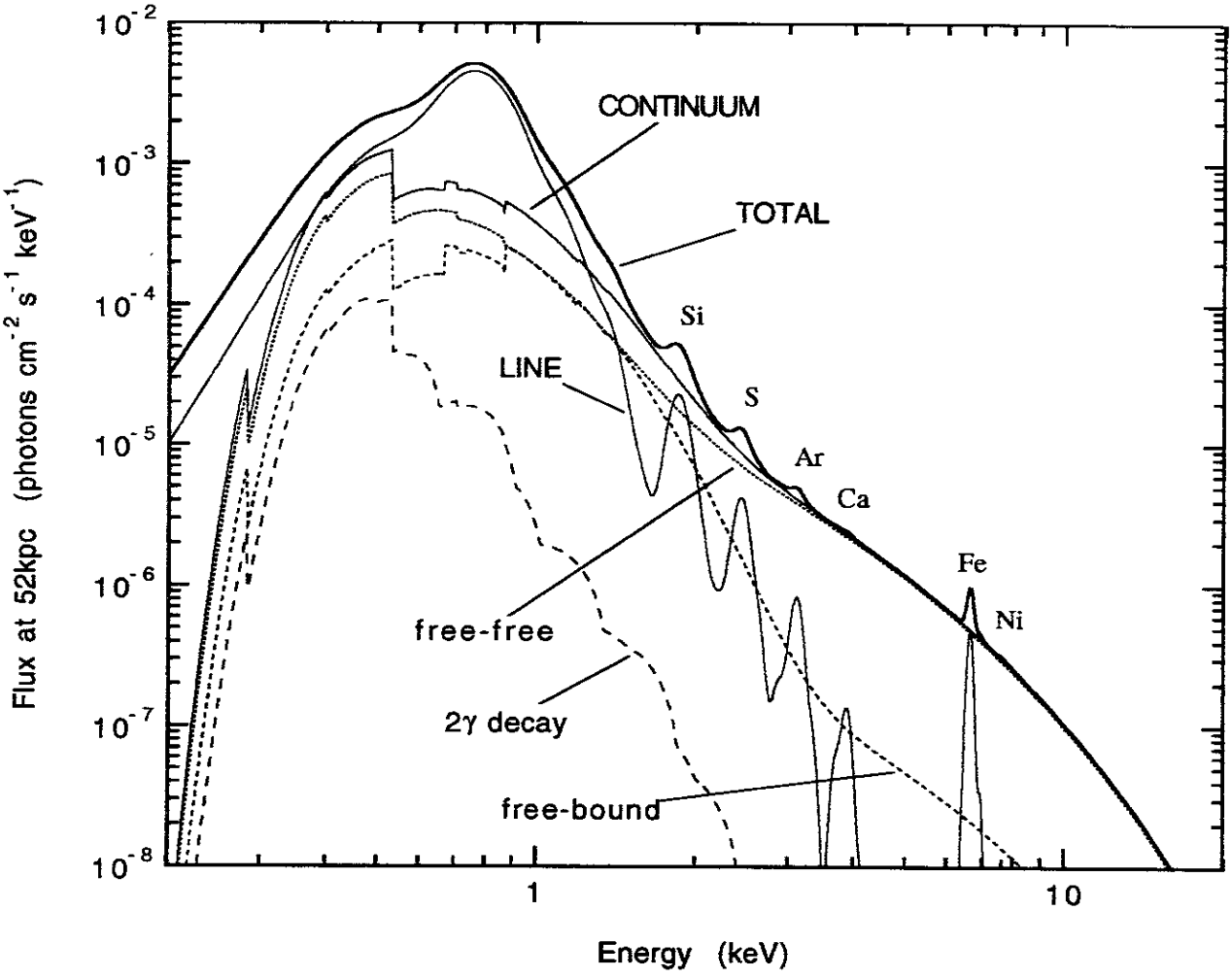
Flux at 52kpc (photons cm^{-2} s^{-1} keV^{-1})
10^{-2}
10^{-3}
10^{-4}
10^{-5}
10^{-6}
10^{-7}
10^{-8}
CONTINUUM
TOTAL
Si
LINE
S
Ar
Ca
Fe
Ni
free-free
2γ decay
free-bound
1
10
Energy (keV)

Fig. 5 (a)

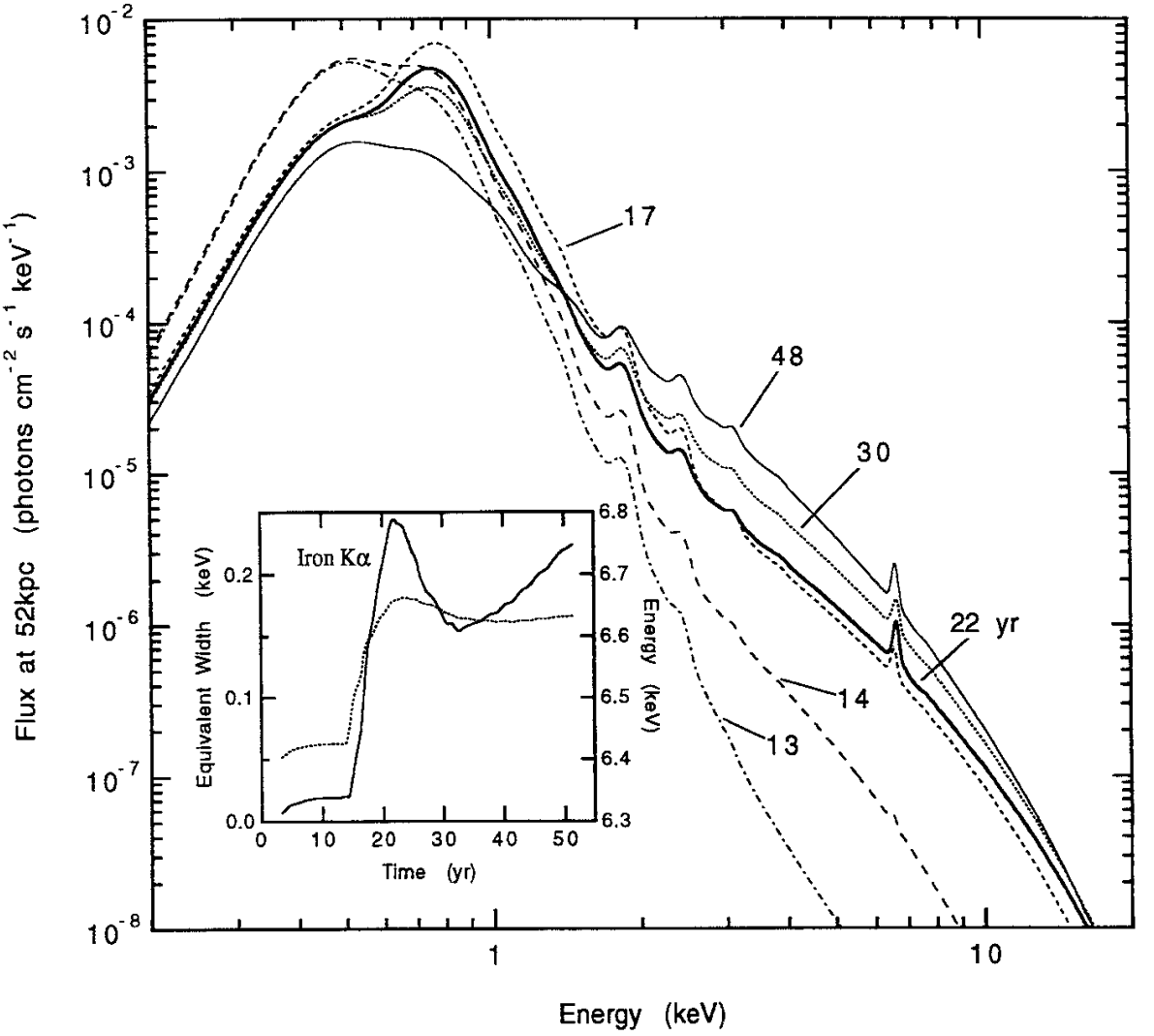
Flux at 52kpc (photons cm^{-2} s^{-1} keV^{-1})
10^{-2}
10^{-3}
10^{-4}
10^{-5}
10^{-6}
10^{-7}
10^{-8}
1
10
Energy (keV)
17
48
30
22 yr
14
13
Iron Kα
Equivalent Width (keV)
0.0
0.1
0.2
0
10
20
30
40
50
Time (yr)
Energy (keV)
6.3
6.4
6.5
6.6
6.7
6.8

Fig. 5(b)

Recent Issues of NIFS Series

NIFS-215 K. Ida, K. Itoh, S.-I.Itoh, Y. Miura, JFT-2M Group and A. Fukuyama, *Thickness of the Layer of Strong Radial Electric Field in JFT-2M H-mode Plasmas*; Apr. 1993

NIFS-216 M. Yagi, K. Itoh, S.-I. Itoh, A. Fukuyama and M. Azumi, *Analysis of Current Diffusive Ballooning Mode*; Apr. 1993

NIFS-217 J. Guasp, K. Yamazaki and O. Motojima, *Particle Orbit Analysis for LHD Helical Axis Configurations* ; Apr. 1993

NIFS-218 T. Yabe, T. Ito and M. Okazaki, *Holography Machine HORN-1 for Computer-aided Retrieve of Virtual Three-dimensional Image* ; Apr. 1993

NIFS-219 K. Itoh, S.-I. Itoh, A. Fukuyama, M. Yagi and M. Azumi, *Self-sustained Turbulence and L-Mode Confinement in Toroidal Plasmas* ; Apr. 1993

NIFS-220 T. Watari, R. Kumazawa, T. Mutoh, T. Seki, K. Nishimura and F. Shimpo, *Applications of Non-resonant RF Forces to Improvement of Tokamak Reactor Performances Part I: Application of Ponderomotive Force* ; May 1993

NIFS-221 S.-I. Itoh, K. Itoh, and A. Fukuyama, *ELMy-H mode as Limit Cycle and Transient Responses of H-modes in Tokamaks* ; May 1993

NIFS-222 H. Hojo, M. Inutake, M. Ichimura, R. Katsumata and T. Watanabe, *Interchange Stability Criteria for Anisotropic Central-Cell Plasmas in the Tandem Mirror GAMMA 10 ;* May 1993

NIFS-223 K. Itoh, S.-I. Itoh, M. Yagi, A. Fukuyama and M. Azumi, *Theory of Pseudo-Classical Confinement and Transmutation to L-Mode;* May 1993

NIFS-224 M. Tanaka, *HIDENEK: An Implicit Particle Simulation of Kinetic-MHD Phenomena in Three-Dimensional Plasmas;* May 1993

NIFS-225 H. Hojo and T. Hatori, *Bounce Resonance Heating and Transport in a Magnetic Mirror;* May 1993

NIFS-226 S.-I. Iton, K. Itoh, A. Fukuyama, M. Yagi, *Theory of Anomalous Transport in H-Mode Plasmas;* May 1993

NIFS-227 T. Yamagishi, *Anomalous Cross Field Flux in CHS ;* May 1993

NIFS-228 Y. Ohkouchi, S. Sasaki, S. Takamura, T. Kato, *Effective Emission and*

Ionization Rate Coefficients of Atomic Carbons in Plasmas; June 1993

NIFS-229 K. Itoh, M. Yagi, A. Fukuyama, S.-I. Itoh and M. Azumi, *Comment on 'A Mean Field Ohm's Law for Collisionless Plasmas;* June 1993

NIFS-230 H. Idei, K. Ida, H. Sanuki, H. Yamada, H. Iguchi, S. Kubo, R. Akiyama, H. Arimoto, M. Fujiwara, M. Hosokawa, K. Matsuoka, S. Morita, K. Nishimura, K. Ohkubo, S. Okamura, S. Sakakibara, C. Takahashi, Y. Takita, K. Tsumori and I. Yamada, *Transition of Radial Electric Field by Electron Cyclotron Heating in Stellarator Plasmas;* June 1993

NIFS-231 H.J. Gardner and K. Ichiguchi, *Free-Boundary Equilibrium Studies for the Large Helical Device,* June 1993

NIFS-232 K. Itoh, S.-I. Itoh, A. Fukuyama, H. Sanuki and M. Yagi, *Confinement Improvement in H-Mode-Like Plasmas in Helical Systems,* June 1993

NIFS-233 R. Horiuchi and T. Sato, *Collisionless Driven Magnetic Reconnection,* June 1993

NIFS-234 K. Itoh, S.-I. Itoh, A. Fukuyama, M. Yagi and M. *Azumi, Prandtl Number of Toroidal Plasmas;* June 1993

NIFS-235 S. Kawata, S. Kato and S. Kiyokawa , *Screening Constants for Plasma;* June 1993

NIFS-236 A. Fujisawa and Y. Hamada, *Theoretical Study of Cylindrical Energy Analyzers for MeV Range Heavy Ion Beam Probes;* July 1993

NIFS-237 N. Ohyabu, A. Sagara, T. Ono, T. Kawamura and O. Motojima, *Carbon Sheet Pumping;* July 1993

NIFS-238 K. Watanabe, T. Sato and Y. Nakayama, *Q-profile Flattening due to Nonlinear Development of Resistive Kink Mode and Ensuing Fast Crash in Sawtooth Oscillations;* July 1993

NIFS-239 N. Ohyabu, T. Watanabe, Hantao Ji, H. Akao, T. Ono, T. Kawamura, K. Yamazaki, K. Akaishi, N. Inoue, A. Komori, Y. Kubota, N. Noda, A. Sagara, H. Suzuki, O. Motojima, M. Fujiwara, A. Iiyoshi, *LHD Helical Divertor;* July 1993

NIFS-240 Y. Miura, F. Okano, N. Suzuki, M. Mori, K. Hoshino, H. Maeda, T. Takizuka, JFT-2M Group, K. Itoh and S.-I. Itoh, *Ion Heat Pulse after Sawtooth Crash in the JFT-2M Tokamak;* Aug. 1993

NIFS-241 K. Ida, Y.Miura, T. Matsuda, K. Itoh and JFT-2M Group, *Observation of non Diffusive Term of Toroidal Momentum Transport in the JFT-*

2M Tokamak; Aug. 1993

NIFS-242 O.J.W.F. Kardaun, S.-I. Itoh, K. Itoh and J.W.P.F. Kardaun,
Discriminant Analysis to Predict the Occurrence of ELMS in H-Mode Discharges; Aug. 1993

NIFS-243 K. Itoh, S.-I. Itoh, A. Fukuyama,
Modelling of Transport Phenomena; Sep. 1993

NIFS-244 J. Todoroki,
Averaged Resistive MHD Equations; Sep. 1993

NIFS-245 M. Tanaka,
The Origin of Collisionless Dissipation in Magnetic Reconnection; Sep. 1993

NIFS-246 M. Yagi, K. Itoh, S.-I. Itoh, A. Fukuyama and M. Azumi,
Current Diffusive Ballooning Mode in Seecond Stability Region of Tokamaks; Sep. 1993

NIFS-247 T. Yamagishi,
Trapped Electron Instabilities due to Electron Temperature Gradient and Anomalous Transport; Oct. 1993

NIFS-248 Y. Kondoh,
Attractors of Dissipative Structure in Three Disspative Fluids; Oct. 1993

NIFS-249 S. Murakami, M. Okamoto, N. Nakajima, M. Ohnishi, H. Okada,
Monte Carlo Simulation Study of the ICRF Minority Heating in the Large Helical Device; Oct. 1993

NIFS-250 A. Iiyoshi, H. Momota, O. Motojima, M. Okamoto, S. Sudo, Y. Tomita, S. Yamaguchi, M. Ohnishi, M. Onozuka, C. Uenosono,
Innovative Energy Production in Fusion Reactors; Oct. 1993

NIFS-251 H. Momota, O. Motojima, M. Okamoto, S. Sudo, Y. Tomita, S. Yamaguchi, A. Iiyoshi, M. Onozuka, M. Ohnishi, C. Uenosono,
Characteristics of D-^{3}He Fueled FRC Reactor: ARTEMIS-L, Nov. 1993

NIFS-252 Y. Tomita, L.Y. Shu, H. Momota,
Direct Energy Conversion System for D-^{3}He Fusion, Nov. 1993

NIFS-253 S. Sudo, Y. Tomita, S. Yamaguchi, A. Iiyoshi, H. Momota, O. Motojima, M. Okamoto, M. Ohnishi, M. Onozuka, C. Uenosono,
Hydrogen Production in Fusion Reactors, Nov. 1993

NIFS-254 S. Yamaguchi, A. Iiyoshi, O. Motojima, M. Okamoto, S. Sudo,

M. Ohnishi, M. Onozuka, C. Uenosono,
Direct Energy Conversion of Radiation Energy in Fusion Reactor,
Nov. 1993

NIFS-255 S. Sudo, M. Kanno, H. Kaneko, S. Saka, T. Shirai, T. Baba,
Proposed High Speed Pellet Injection System "HIPEL" for Large Helical Device
Nov. 1993

NIFS-256 S. Yamada, H. Chikaraishi, S. Tanahashi, T. Mito, K. Takahata, N. Yanagi, M. Sakamoto, A. Nishimura, O. Motojima, J. Yamamoto, Y. Yonenaga, R. Watanabe,
Improvement of a High Current DC Power Supply System for Testing the Large Scaled Superconducting Cables and Magnets; Nov. 1993

NIFS-257 S. Sasaki, Y. Uesugi, S. Takamura, H. Sanuki, K. Kadota,
Temporal Behavior of the Electron Density Profile During Limiter Biasing in the HYBTOK-II Tokamak; Nov. 1993

NIFS-258 K. Yamazaki, H. Kaneko, S. Yamaguchi, K.Y. Watanabe, Y.Taniguchi, O.Motojima, LHD Group,
Design of Central Control System for Large Helical Device (LHD);
Nov. 1993

NIFS-259 K. Yamazaki, H. Kaneko, S. Yamaguchi, K.Y. Watanabe, Y.Taniguchi, O.Motojima, LHD Group,
Design of Central Control System for Large Helical Device (LHD);
Nov. 1993

NIFS-260 B.V.Kuteev,
Pellet Ablation in Large Helical Device; Nov. 1993

NIFS-261 K. Yamazaki,
Proposal of "MODULAR HELIOTRON': Advanced Modular Helical System Compatible with Closed Helical Divertor; Nov. 1993

NIFS-262 V.D.Pustovitov,
Some Theoretical Problems of Magnetic Diagnostics in Tokamaks and Stellarators; Dec. 1993

NIFS-263 A. Fujisawa, H. Iguchi, Y. Hamada
A Study of Non-Ideal Focus Properties of 30° Parallel Plate Energy Analyzers; Dec. 1993

NIFS-264 K. Masai,
Nonequilibria in Thermal Emission from Supernova Remnants;
Dec. 1993